Polymer 51 (2010) 1555–1562

Contents lists available at ScienceDirect

Polymer

journal homepage: www.elsevier.com/locate/polymer

Synthesis and optoelectronic properties of luminescent copolyfluorenes slightly doped with thiophene chromophore

Wen-Fen Su, Tsui-Ting Chen, Yun Chen*

Department of Chemical Engineering, National Cheng Kung University, Tainan, Taiwan

A R T I C L E I N F O

Article history:
Received 2 December 2009
Received in revised form
3 February 2010
Accepted 5 February 2010
Available online 12 February 2010

Keywords:
Copolyfluorenes
Electroluminescence
Charge trapping

A B S T R A C T

This paper describes the synthesis of new copolyfluorenes (**P05**–**P5**) slightly doped with 2,5-bis(2-phenyl-2-cyanovinyl)thiophene (**GM**, <3.4 mol%) and their application in electroluminescent (EL) devices. In film state, EL spectra of the copolyfluorenes are very different from photoluminescence (PL) spectra, which have been ascribed to charge trapping in **GM** and energy transfer from fluorene segments to **GM** chromophores. The maximum brightness and current efficiency of EL device from **P05** (5230 cd/m^2, 0.65 cd/A) are significantly enhanced when compared with those from poly(9,9-dihexylfluorene) (**PF**) (1310 cd/m^2, 0.18 cd/A). The EL device using blend of **P5** and **PF** ($w/w = 10/1$) as emitting layer exhibits near-white emission with CIE coordinate being (0.26, 0.32). The results demonstrate that the copolyfluorenes slightly doped with **GM** chromophore are promising emitting materials for optoelectronic devices.

1. Introduction

In the last two decades, the synthesis of light-emitting polymers have received intense attention after the discovery of electroluminescence (EL) in conjugated polymers and the development of polymer-light-emitting diodes (PLEDs) as display and lighting applications [1–3]. A lot of conjugated polymers, such as poly(*p*-phenylenevinylene) (PPV) [1], polythiophene (PT) [4], poly(*p*-phenylene) (PPP) [5], and polyfluorene (PF) [6], and their derivatives have been extensively investigated. Polythiophene (PT) and its derivatives are promising candidates for electrically conductive and optoelectronic materials due to their narrow band-gap, high stability, high electrical conductivity, and attractive electronic and optical properties [4,7–9]. Nevertheless, relatively low photoluminescence (PL) quantum efficiency of PT in the solid state [10], typically 1–3% [11], has limited their applications in PLEDs. Hence, PT with modified backbone structures by introducing phenylene [12] and fluorene [13] groups were developed. It was reported that for a dioctyl-phenyl substituted polythiophene derivative the PL efficiency can be improved to 24% [11,14]; Liu et al. reported a series of fluorene–thiophene copolymers showing PL efficiency in the range of 23–40% [13]. Pei et al. increased the quantum efficiency of polythiophene by incorporating fluorene moiety into backbone [15]. Furthermore, the thiophene units had been incorporated into polyfluorene backbone to adjust band-gap and to tune emission color [12,13,16–23]. The π-excessive thiophene ring reduced oxidation potential of the fluorene moiety [24], which in turn raised HOMO level of the copolyfluorenes to promote hole-injection. Cho et al. further incorporated cyano group (CN) to prepare a series copolyfluorenes containing red-emitting chromophore – 2,5-bis(2-(5′-bromothienyl)-1-cyanovinyl)-1-(2″-ethylhexyloxy)-4-methoxybenzene [25,26], and found that substitution of thiophene by phenylene resulted in improved EL device performance.

Polyfluorene (PF) and its derivatives are attractive blue-emitting materials for PLEDs application because of their thermal, chemical stability and high photoluminescence (PL) efficiency in solution and solid states [27–30]. However, PF shows imbalance in charges (electron and hole) injection and mobility when utilized as emitting materials. This characteristic leads to low efficiency in its polymeric light-emitting diodes (PLEDs), and because of this, numerous attempts have been made to improve their performance [16,21,31]. Meanwhile, the PFs with large band-gap can be used as host material to blend with low band-gap chromophores. Furthermore, fluorene can copolymerize with chromophores having different band-gaps to obtain various emission colors. For example, red-light emissions with CIE at (0.63, 0.37) were obtained by copolymerizing fluorene with narrow band-gap monomer [31].

In this investigation, we designed a series of copolyfluorenes containing a new low band-gap chromophore – 2,5-bis(2-phenyl-2-cyanovinyl)thiophene (**GM**). The chromophore contains only one thiophene core that is attached with two 2-phenyl-2-cyanovinyl groups. By this way, the content of heavy-atom (sulfur) can be

---

* Corresponding author. Tel.: +886 6 2085843; fax: +886 6 2344496.
E-mail address: yunchen@mail.ncku.edu.tw (Y. Chen).

0032-3861/$ – see front matter © 2010 Elsevier Ltd. All rights reserved.
doi:10.1016/j.polymer.2010.02.012

reduced to enhance emitting performance. The resulting copolyfluorene (**P05**–**P5**) are slightly doped with **GM** chromophores (<3.4 mol%). The copolymers exhibited yellowish-green electroluminescence (EL) due to overwhelming energy transfer from fluorene segments to **GM** chromophores when its content was 2.3 mol%. The performances of EL devices using the copolyfluorenes as active layer surpassed that fabricated from **PF**. Doped **GM** chromophores also act as charge trapping sites to promote the recombination of holes and electrons, which is an essential step in EL processes. Besides, near-white-light emission is obtainable by blending of the copolyfluorenes with poly(9,9-dihexylfluorene) (**PF**).

2. Materials and methods

2.1. Materials and characterization

4-Bromophenylacetonitrile (Lancaster Co.), phenylacetonitrile (TCI Co.), 9,9-dihexyl-2,7-dibromofluorene (Aldrich Co.), 9,9-dihexylfluorene-2,7-bis(trimethyleneborate) (Aldrich Co.), Aliquat 336 (Alfa Aesar Co.), tetrakis(triphenylphosphine)palladium [$\mathrm{Pd(PPh_3)_4}$] (Acros Co.), methanol (ECHO Co.), toluene (Tedia Co.), chloroform ($\mathrm{CHCl_3}$, Tedia Co.) and other solvents were HPLC grade reagents. All reagents and solvents were used without further purification. All compounds were identified by ^{1}H NMR, ^{13}C NMR, Fourier transform infrared (FT-IR), and elemental analysis (EA). NMR spectra were obtained on a Bruker AVANCE-400 NMR spectrometer with chemical shifts reported in ppm using tetramethylsilane (TMS) as an internal standard. The FT-IR spectra were measured as KBr disk using a Fourier transform infrared spectrometer, model 7850 from Jasco. The elemental analysis was carried out on a Heraus CHN-Rapid elemental analyzer. The molecular weight and molecular weight distribution of the copolymers were determined by a gel permeation chromatograph (GPC) using chloroform ($\mathrm{CHCl_3}$) as eluent. The thermogravimetric analysis (TGA) of the polymers was performed under nitrogen atmosphere at a heating rate of 10 °C/min using a PerkinElmer TGA-7 thermal analyzer. Thermal properties of the polymers were measured using a differential scanning calorimeter (DSC), Mettler Toledo DSC 1 Star System, under nitrogen atmosphere at a heating rate of 10 °C/min. Absorption spectra were measured with a Jasco V-550 spectrophotometer and the photoluminescence (PL) spectra were obtained using a Hitachi F-4500 fluorescence spectrophotometer. The cyclic voltammograms of the polymers were measured with a voltammetric apparatus (model CV-50W from BAS) equipped with a three-electrode cell. The cell was made up of a polymer-coated glassy carbon as the working electrode, an Ag/AgCl electrode as the reference electrode, and a platinum wire as the auxiliary electrode, immersing in acetonitrile containing 0.1 M (n-Bu)$_4$NClO$_4$. The energy levels were calculated using the ferrocene (FOC) value of −4.8 eV with respect to vacuum level, which is defined as zero [32]. Morphology image of the polymers' film were captured using atomic force microscope, Veeco/Digital Instrument Scanning Probe Microscope (tapping mode) with Nanoscope IIIa controller. The polymer solution (12 mg/mL in chlorobenzene) was prepared and filtered with a syringe filter (0.22-ìm pore) to remove possible particle contaminants, and then spin-coated on the top of cleaned ITO glass.

*2.2. Synthesis of model compound **GM** and monomer **M1** (Scheme 1)*

*2.2.1. 2,5-Bis(2-phenyl-2-cyanovinyl)thiophene (**GM**)*

The new monomer **M1** and model compound **GM** were synthesized by modifying the procedures described in previous literatures [25,29,33,34]. For example, a mixture of 2,5-thiophenedicarboxaldehyde (**2**: 0.14 g, 1 mmol) and phenylacetonitrile (**1**: 0.588 g, 3 mmol) in 10 mL methanol was stirred at room temperature under nitrogen atmosphere. After complete dissolution of the solids, it was added dropwise with an ethanol solution of sodium ethoxide (21%) and allowed to react for 12 h. The appearing precipitates were collected by filtration, washed successively with distilled water and hydrochloric acid. The solids were recrystallized from ethyl acetate and n-hexane to give orange solids of **GM**. The yield was 63% (mp = 169–170 °C). FT-IR (KBr pellet, cm^{-1}): ν 532, 685, 760, 809, 1236, 1448, 1498, 1587, 2210 (−C≡N), 3035, 3057. ^{1}H NMR ($\mathrm{CDCl_3}$, 400 MHz, ppm): δ 7.38–7.47 (m, 6H, Ar–$\underline{\mathrm{H}}$), 7.61 (s, 2H, Ar–$\underline{\mathrm{H}}$), 7.66–7.68 (d, 4H, Ar–$\underline{\mathrm{H}}$, $J = 8$ Hz), 7.80 (s, 2H, −C$\underline{\mathrm{H}}$−). ^{13}C NMR ($\mathrm{CDCl_3}$, 400 MHz, ppm): δ 110.64, 117.84, 125.83, 128.98, 129.21, 129.51, 129.77, 130.32, 131.94, 132.49, 133.43, 133.86, 136.44, 140.97. ELEM. ANAL. Calcd. for $\mathrm{C_{22}H_{14}N_2S}$ (%): C, 78.08; H, 4.17; N, 8.28; S, 9.47. Found: C, 78.00; H, 4.14; N, 8.27; S, 9.50.

*2.2.2. 2,5-Bis[2-(4′-bromophenyl)-2-cyanovinyl]thiophene (**M1**)*

The synthetic procedures were analogous to those employed in the preparation of **GM** with the exception of using 4-bromophenylacetonitrile (**3**) instead of phenylacetonitrile (**1**), and the product was orange solid. The yield was 72% (mp = 225–226 °C). FT-IR (KBr pellet, cm^{-1}): ν 76, 538, 823, 1072, 1234, 1402, 1483, 1587, 2208 (−C≡N), 3035, 3089. ^{1}H NMR ($\mathrm{CDCl_3}$, 400 MHz, ppm): δ 7.51–7.65 (m, 10H, Ar–$\underline{\mathrm{H}}$), 7.81 (s, 2H, −C$\underline{\mathrm{H}}$−). ^{13}C NMR ($\mathrm{CDCl_3}$, 400 MHz, ppm): δ 106.74, 114.06, 120.05, 128.92, 129.20, 129.28, 129.40, 137.85. ELEM. ANAL. Calcd. for $\mathrm{C_{22}H_{12}Br_2N_2S}$ (%): C, 53.25; H, 2.44; N, 5.65; S, 6.46. Found: C, 53.19; H, 2.51; N, 5.65; S, 6.55.

2.3. Polymer synthesis (Scheme 2) [35]

Poly(9,9-dihexylfluorene) (**PF**) and copolyfluorenes (**P05**–**P5**) were prepared from monomer **4**, **5**, and **M1** by the palladium-catalyzed Suzuki coupling reaction. The feed ratios of **M1** were 0% and 0.5–5 mol% for **PF** and **P05**–**P5**, respectively. The general synthetic procedures of the copolyfluorenes are described as follows: 9,9-dihexylfluorene-2,7-bis(trimethyleneborate) (**4**), 9,9-dihexyl-2,7-dibromofluorene (**5**), monomer **M1**, $\mathrm{(PPh_3)_4Pd(0)}$ and several drops of Aliquat 336 were added to a mixture consisting of toluene and aqueous solution of $\mathrm{K_2CO_3}$ (2 M). The mixture was first purged with nitrogen and then stirred rigorously at 90 °C for 72 h. Then extra **4** and bromobenzene were successively added to end-cap the polymer chain. After cooling to room temperature, the mixture was poured into a large quantity of methanol and distilled water ($v/v = 10/1$). The appearing solid was collected by filtration and washed thoroughly with methanol, followed by Soxhlet extraction with acetone to remove trace oligomers and catalyst residues.

PF: FT-IR (KBr pellet, cm^{-1}): ν 1458 (−C=C−), 2858, 2927, 2951 ($-\mathrm{CH_2}-$). ^{1}H NMR ($\mathrm{CDCl_3}$, 400 MHz, ppm): δ 0.76–0.81 (m, 10H, $-\mathrm{C\underline{H}_2C\underline{H}_3}$), 1.14 (s, 12H, $-\mathrm{C\underline{H}_2}-$), 2.12 (s, 4H, $-\mathrm{C\underline{H}_2}-$), 7.67 (s, 4H, Ar–$\underline{\mathrm{H}}$), 7.83–7.86 (d, 2H, Ar–$\underline{\mathrm{H}}$, $J = 12$ Hz). ELEM. ANAL. Calcd. for $\mathrm{C_{25}H_{32}}$ (%): C, 90.30; H, 9.63. Found: C, 89.56; H, 9.76.

P05: FT-IR (KBr pellet, cm^{-1}): ν 1460 (−C=C−), 2856, 2927, 2952 ($-\mathrm{CH_2}-$), 2213 (−CN). ^{1}H NMR ($\mathrm{CDCl_3}$, 400 MHz, ppm): δ 0.78–0.81 (t, 10H, $-\mathrm{C\underline{H}_2C\underline{H}_3}$, $J = 12$ Hz), 1.14 (s, 12H, $-\mathrm{C\underline{H}_2}-$), 2.12 (s, 4H, $-\mathrm{C\underline{H}_2}-$), 7.67–7.70 (m, 4H, Ar–$\underline{\mathrm{H}}$), 7.83–7.85 (m, 2H, Ar–H). ELEM. ANAL. found for $\mathrm{C_{49}H_{50}N_2S}$: C, 89.39%; H, 9.58%; N, <0.1%; S, <0.1%.

P1: FT-IR (KBr pellet, cm^{-1}): ν 1458 (−C=C−), 2854, 2927, 2952 ($-\mathrm{CH_2}-$), 2213 (−CN). ^{1}H NMR ($\mathrm{CDCl_3}$, 400 MHz, ppm): δ 0.76–0.81 (t, 10H, $-\mathrm{C\underline{H}_2C\underline{H}_3}$, $J = 20$ Hz), 1.14–1.25 (d, 12H, $-\mathrm{C\underline{H}_2}-$, $J = 44$ Hz), 2.13 (s, 4H, $-\mathrm{C\underline{H}_2}-$), 7.67–7.71 (m, 4H, Ar–$\underline{\mathrm{H}}$), 7.83–7.85 (m, 2H, Ar–$\underline{\mathrm{H}}$). ELEM. ANAL. found for $\mathrm{C_{49}H_{50}N_2S}$: C, 88.38%; H, 9.48%; N, <0.10%; S, <0.20%.

P3: FT-IR (KBr pellet, cm^{-1}): ν 1458 (−C=C−), 2854, 2927, 2951 ($-\mathrm{CH_2}-$), 2212 (−CN). ^{1}H NMR (CDCl3, 400 MHz, ppm): δ 0.78–0.81 (t, 10H, $-\mathrm{C\underline{H}_2C\underline{H}_3}$, $J = 12$ Hz), 1.14–1.25 (d, 12H, $-\mathrm{C\underline{H}_2}-$, $J = 44$ Hz), 2.12 (s, 4H, $-\mathrm{C\underline{H}_2}-$), 7.67–7.71 (m, 4H, Ar–$\underline{\mathrm{H}}$), 7.84–7.86 (m, 2H,

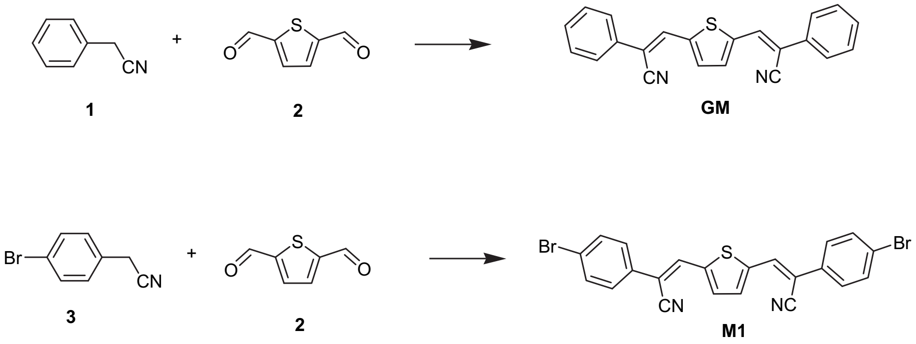

Scheme 1. Synthetic procedures of monomer **M1** and model compound **GM**.

Ar–$\underline{H}$). E_{LEM}. A_{NAL}. found for $C_{49}H_{50}N_2S$: C, 87.31%; H, 9.28%; N, 0.21%; S, 0.22%.

P5: FT-IR (KBr pellet,cm^{-1}): ν 1460 (–C=C–), 2854, 2927, 2952 (–CH_2–), 2211 (–CN). ^{1}H NMR ($CDCl_3$, 400 MHz, ppm): δ 0.78–0.80 (d, 10H, –$C\underline{H}_2C\underline{H}_3$, $J = 8$ Hz), 1.14–1.33 (m, 12H, –$C\underline{H}_2$–), 2.12 (s, 4H, –$C\underline{H}_2$–), 7.48–7.67 (m, 4H, Ar–$\underline{H}$), 7.83–7.85 (m, 2H, Ar–$\underline{H}$). E_{LEM}. A_{NAL}. found for $C_{49}H_{50}N_2S$: C, 87.63%; H, 9.21%; N, 0.26%; S, 0.32%.

2.4. Fabrication and characterization of EL devices

Light-emitting devices (ITO/PEDOT:PSS/polymer/Ca/Al) were fabricated by successive coating of hole-injection layer (PEDOT:PSS) and active layer (emitting polymer) onto transparent conductive ITO glass, followed by vacuum deposition of calcium and aluminum as cathode. The ITO glasses were pre-cleaned consecutively with ultrasonic bath in neutraler reiniger/de-ionized water (1:10 volume) mixture, de-ionized water, acetone and 2-propanol, and then dried *in vacuo*. The PEDOT:PSS was first spin-coated on top of cleaned ITO glass and dried at 150 °C for 15 min. The polymer solution (12 mg/mL in chlorobenzene) was prepared and filtered with a syringe filter (0.22-ìm pore) to remove possible particle contaminants, and then spin-coated onto the PEDOT:PSS layer to form as the emitting layer. Finally, a thick layer of Ca (*ca.* 50 nm) and Al (*ca.* 100 nm) were consecutively deposited as a cathode by thermal evaporation under a vacuum of 2×10^{-6} Torr. The EL spectra and luminance–current–voltage characteristics of the devices were recorded using a combination of Keithley power source (model 2400) and Ocean Optics usb2000 fluorescence spectrophotometer.

3. Results and discussion

3.1. Synthesis and characterization

The synthetic schemes of dibromo monomer (**M1**) and model compound of green chromophore (**GM**) are shown in Scheme 1 [25,29,33,34]. Monomer **M1** and model **GM** were prepared with high yields according to reported procedures and had been well characterized. Poly(9,9-dihexylfluorene) (**PF**) and copolyfluorenes **P05**–**P5** were synthesized by the Suzuki coupling reaction using Pd$(PPh_3)_4$ as the catalyst and Aliquat 336 as the phase-transfer reagent in a mixture of toluene and aqueous K_2CO_3 (Scheme 2). The feed ratios of monomer **M1** in the preparation of copolymers **P05**, **P1**, **P3** and **P5** were 0.5 mol%, 1 mol%, 3 mol% and 5 mol%, respectively. Monomer **4** and mono-functional bromobenzene were used as the end-capping agents after the polymerization. Chemical structures of **PF** and **P05**–**P5** were identified by ^{1}H NMR, FT-IR spectra, and elemental analysis data. The ^{1}H NMR spectra of the copolyfluorenes are similar to that of polyfluorene (**PF**) due to low incorporated contents of the **GM** chromophore. Accordingly, chromophore contents of **P3** and **P5** were estimated from elemental analysis (EA) data (Table 1) to be 2.3 mol% and 3.4 mol%, which are lower than feed compositions (3 mol% and 5 mol% respectively). Clearly, the copolymerization reactivity of **M1** is lower than 9,9-dihexyl-2,7-dibromofluorene (**5**). However, the composition estimation of **P05** and **P1** was not successful because their contents of nitrogen and sulfur were lower than detection limit of the EA instrument. The FT-IR spectra of **PF** and **P05**–**P5** show characteristic vibration band of cyano group at 2213 cm^{-1}, whose intensity is gradually enhanced with increasing **GM** contents. All polymers are soluble in common organic solvents such as toluene, chloroform and chlorobenzene. The weight-average molecular weights (M_w) of **PF** and **P05**–**P5**, determined by GPC using mono-disperse polystyrenes as a calibration standard, are in the range of 2.4×10^4–4.2×10^4, with polydispersity index (PDI) being between 2.0 and 2.8 (Table 1). Thermogravimetric analysis (TGA) and differential scanning calorimetry (DSC) were employed to investigate thermal behaviors of the polymers. As shown in Table 1, the thermal decomposition temperature (T_d) of **PF** and copolyfluorenes **P05**–**P5** are higher than 410 °C. The residual weights of **PF** and copolyfluorenes **P05**–**P5** at 800 °C in air were 1.3–4.5%, suggesting

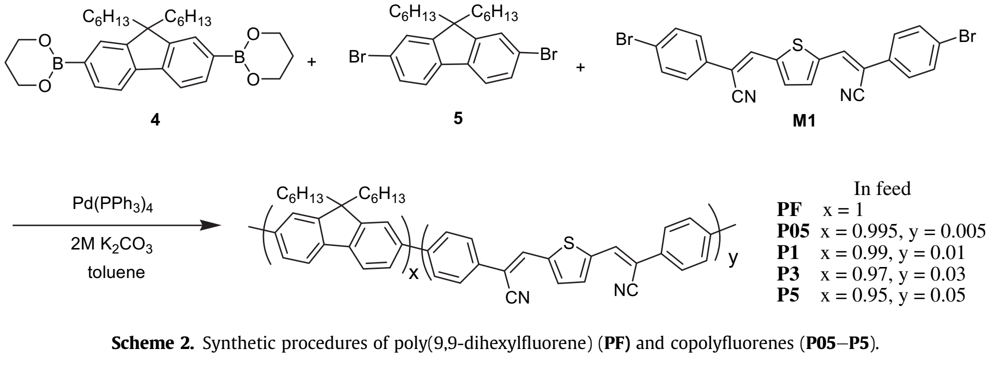

Scheme 2. Synthetic procedures of poly(9,9-dihexylfluorene) (**PF**) and copolyfluorenes (**P05**–**P5**).

Table 1
Polymerization results and characterization of the polymers.

	Yield (%)	M_n[a] ($\times 10^4$)	M_w[a] ($\times 10^4$)	PDI[a]	T_g (°C)[b]	T_d (°C)[c]	y (%)[d]	W_R (%)[f]
PF	70	1.83	4.18	2.28	96	421	0	51.6(2.6)
P05	71	1.47	2.91	1.98	94	420	–[e]	50.8(4.1)
P1	72	1.08	2.39	2.21	94	417	–[e]	52.1(4.5)
P3	73	1.04	2.66	2.56	97	410	2.3	51.2(1.3)
P5	72	1.01	2.84	2.81	107	410	3.4	49.7(4.4)

[a] M_n, M_w, and PDI of the polymers were determined by gel permeation chromatography using polystyrene standards in $CHCl_3$.
[b] Glass transition temperature (T_g) was measured by DSC at a heating rate of 10 °C/min.
[c] Thermal decomposition temperature (T_d) at 5 wt% loss under nitrogen atmosphere.
[d] The y values were actual molar percent of the **GM** chromophore in the copolyfluorenes, estimated from elemental analysis (EA) data.
[e] Lower than measuring limit of the EA instrument.
[f] Residual weight: remaining weight of the polymers upon heating to 800 °C in nitrogen atmosphere; the values in the parentheses are those in air.

that slight carbonization might occur at high temperature. Furthermore, the glass transition temperatures (T_g) of **PF** and **P05**–**P5** increase gradually from 94 °C to 107 °C with an increase in **GM** composition. When fabricated as emitting layer in PLEDs, emitting polymer with higher T_g is conducive to suppress morphology deformation and degradation under high driving voltage.

3.2. *Optical properties*

Model compound **GM** was prepared to investigate the energy transfer between fluorene segment and chromophore. As shown in Fig. 1, the absorption peak of **GM** locates at 404 nm; the main emission situates at 475 nm with a shoulder at *ca.* 500 nm. Homopolyfluorene **PF** shows absorption and emission peaks at 387 nm and 419 nm, respectively. The absorption band of **GM** overlaps extensively with the emission band of **PF**; therefore efficient energy transfer from fluorene segment to **GM** chromophore can be reasonably expected [26]. The optical properties of **GM** and copolymers are summarized in Table 2. In solution state, the absorption and PL spectra of **P05**–**P5** show peaks at *ca.* 387 and 419 nm, respectively, which are contributed exclusively from fluorene segments. Moreover, both absorption and PL spectra of **P05**–**P5** are very similar to those of **PF** (Fig. S1 in Supporting information), which is attributable to slight composition of **GM** chromophore in main chain. Furthermore, their absorption spectra in the film state are qualitatively similar to those in solution; the only difference is slight enhancement of absorption at *ca.* 400–440 nm region with increasing **GM** contents. However, the absorption peak reveals slight blue-shift (from 387 nm to 379 nm) in going from solution to film state (Table 2). This is ascribed to chain entanglement in film state as a result of concentrated polymer solution used in film casting (12 mg polymer/1 mL chloroform). In our previous study, we found that the absorption maxima were blue-shifted from 391 to 369 nm when the concentration was increase from 6 to 30 mg/1 mL [36].

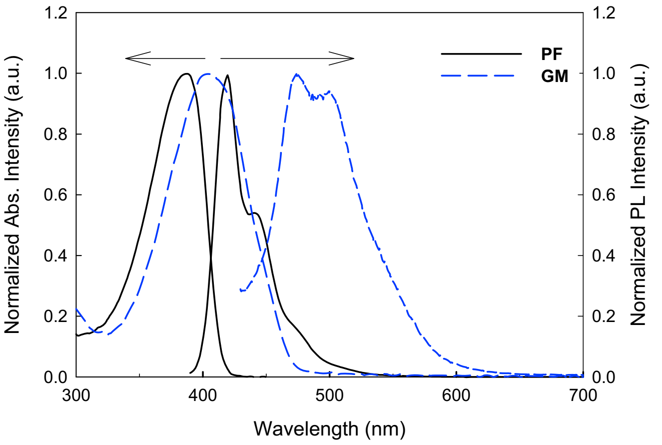

Fig. 1. Absorption and photoluminescence (λ_{ex}: 385 nm) spectra of **PF** and **GM** in $CHCl_3$ solution.

Fig. 2 shows film state photoluminescence (PL) spectra of **PF** and **P05**–**P5**, in which the main emissions at *ca.* 425 nm and 535 nm are attributed to fluorene segments and **GM** chromophores, respectively. The solid state PL spectra of **P3** and **P5** containing high **GM** contents (2.3 mol% and 3.4 mol%) are very different from those in solution. The emission intensity at 535 nm is enhanced dramatically, accompanied with simultaneous degeneration of emission at 425 nm. This enhancement of green emission is due to efficient Förster energy transfer from fluorene segments to **GM** chromophores, occurring intra- and intermolecularly in film state [21]. The phenomenon is quite common in copolymers containing narrow band-gap chromophores [26,37]. Moreover, the PL quantum efficiencies of the copolyfluorenes are decreased from 0.86 (**P05**) to 0.52 (**P5**) with increasing **GM** contents (Table 2), estimated using **PF** as reference standard ($\Phi_{PL} = 1$). The heavy-atom sulfur in **GM** chromophore inevitably increases the intersystem crossing process from singlet state and triplet state that degrades PL efficiency.

3.3. *Electrochemical properties* [38,39]

Cyclic voltammetry was used to investigate the reduction–oxidation behaviors of the copolyfluorenes to comprehend their electrochemical properties. The HOMO and LUMO energy levels of the polymer films can be estimated from the cyclic

Table 2
Optical properties of **GM** and copolymers.

	Solution[a]			Film		
	UV–vis λ_{max} (nm)	PL λ_{max} (nm)[b]	$\sqrt{\phi_{PL}}$	UV–vis λ_{max} (nm)	PL λ_{max} (nm)[b]	Stokes shift (nm) [c]
GM	404	475,500	–	–	–	–
PF	387	419, 441	1	379	426, 451, 481	47
P05	386	419, 441	0.86	379	425, 454,483	47
P1	387	419, 441	0.85	379	425, 451, 483	47
P3	387	419, 441	0.58	379	425, 451, 535	157
P5	387	419, 441	0.52	381	425, 451, 539	161

[a] In chloroform (1×10^{-5} M).
[b] The excitation wavelength was 385 nm.
[c] Stokes shift = PL(film)/nm – UV(film)/nm.

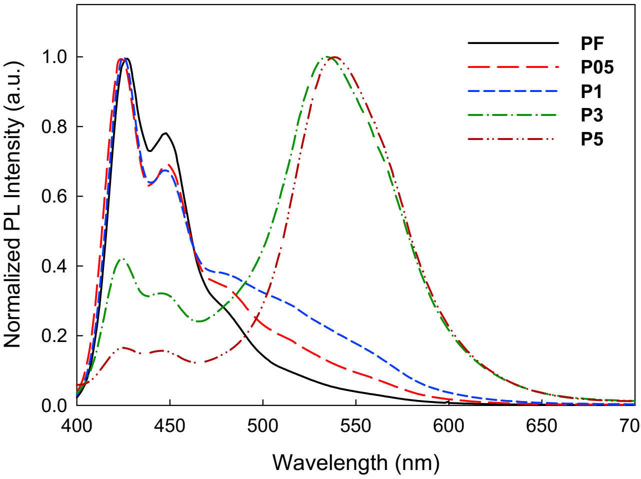

Fig. 2. Photoluminescence spectra (λ_{ex}: 385 nm) of **PF** and copolyfluorenes **P05**–**P5** in the film state.

voltammograms (CV) using the equations $E_{HOMO} = -(E_{ox} + 4.8)$ eV and $E_{LUMO} = -(E_{red} + 4.8)$ eV, respectively, where E_{ox} and E_{red} are the onset oxidation and onset reduction potentials, respectively, relative to the ferrocene/ferrocenium couple. The polymer films coated on a glassy carbon working electrode, supported in 0.10 M tetra-*n*-butylammonium perchlorate ($(n\text{-Bu})_4NClO_4$) in anhydrous acetonitrile, were measured at a scanning rate of 100 mV/s. The cyclic voltammograms of **GM**, **PF** and **P5** are shown in the Fig. S2 and the corresponding electrochemical data are summarized in Table 3. The HOMO and LUMO levels of **GM** are estimated to be −5.62 and −3.41 eV, respectively, from which the electrochemical band-gap (E_g^{el}) of **GM** is estimated to be 2.21 eV. The estimated LUMO levels of the copolyfluorenes (**P05**–**P5**) decrease from −2.77 eV to −2.89 eV with an increase in **GM** contents (to 3.4 mol %). The LUMO levels are lower than −2.73 eV of **PF**. On the contrary, the HOMO levels remain almost unchanged at −5.64 eV, which are close to −5.66 eV of **PF**. Therefore, by incorporating **GM** chromophores, consisting of narrow band-gap thiophene and electron affinitive cyano groups, the band-gap of copolyfluorenes decreases from 2.93 eV (**PF**) to 2.75 eV (**P5**) [40]. However, the LUMO level of **GM** (−3.41 eV) is much lower than that of **PF** (−2.73 eV); therefore, the energy barrier of electron injection can be effectively reduced by the incorporation of **GM** chromophore [40]. Fig. 3 shows the energy band diagrams of **PF** and **GM**. The HOMO and LUMO levels of **GM** lie between those of **PF**, suggesting that **GM** chromophore acts as a charge trapping site for the copolyfluorenes [21]. Therefore, electrons and holes tend to recombine mainly in **GM** chromophores and charge trapping could be the major mechanism for the EL process.

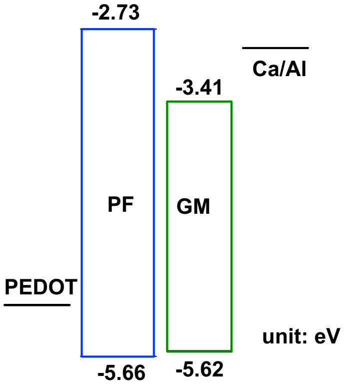

Fig. 3. Energy level diagrams of **PF** and **GM**.

3.4. Electroluminescent properties

Double-layer electroluminescent (EL) devices having a structure of ITO/PEDOT:PSS/emitting layer/Ca(50 nm)/Al(100 nm) were fabricated to investigate the optoelectronic properties and performances of the copolyfluorenes. Fig. 4 shows the current density versus bias and brightness versus bias curves (*J*–*B*–*V*) of the EL devices, with the corresponding characteristic data summarized in Table 4. The turn-on voltages (at 10 cd/m^2) are in the range of 5.3–7.8 V; the maximum brightness and maximum current efficiency are 2000–5230 cd/m^2 and 0.43–0.65 cd/A, respectively. The brightness–voltage–luminance (*B*–*V*) curves shift to higher voltages with increasing **GM** composition, suggesting that the **GM** chromophores dominate the charge trapping processes [21]. Both maximum brightness and maximum current efficiency of **P05**–**P5** are superior to those of **PF** (1310 cd/m^2, 0.18 cd/A). The **P05** device exhibits the best performance, with the maximum brightness and current efficiency being 5230 cd/m^2 and 0.65 cd/A, respectively. Clearly, incorporating small amount of **GM** chromophore significantly enhances the device performance. This is attributable to enhanced recombination of electrons and holes at **GM** chromophore which act as charge trapping sites. Hence, our device results obviously demonstrate that **GM** chromophore can increase maximum brightness of the EL devices. However, the brightness of **P05**–**P5** devices decrease from 5230 cd/m^2 (**P05**) to 2000 cd/m^2 (**P5**) as **GM** content on the backbone increases, due mainly to the heavy-atom effect (sulfur in **GM** chromophore) [41]. Therefore, it is necessary to control **GM** contents to obtain efficient EL devices. The AFM images of the films cast from **PF** and copolyfluorenes **P05**–**P5**, in which the root-mean-square (rms) roughness of the copolyfluorenes increases from 1.24 to 1.83 with increasing **GM** contents (Fig. S3). Therefore, both rough morphology and heavy-atom effect degrade device brightness and efficiency at high **GM** contents.

Table 3
Electrochemical potentials of the **GM** and copolymers.

Polymer	$E_{onset(ox)}$ *vs.* FOC (V)[a]	$E_{onset(red)}$ *vs.* FOC (V)[a]	E_{HOMO} (eV)[b]	E_{LUMO} (eV)[b]	E_g^{el} (eV)[c]	E_g^{opt} (eV)[d]
GM	0.82	−1.39	−5.62	−3.41	2.21	–
PF	0.86	−2.07	−5.66	−2.73	2.93	2.93
P05	0.84	−2.03	−5.64	−2.77	2.87	2.95
P1	0.84	−2.01	−5.64	−2.79	2.85	2.93
P3	0.84	−2.00	−5.64	−2.80	2.84	2.93
P5	0.84	−1.91	−5.64	−2.89	2.75	2.83

[a] $E_{FOC} = 0.47$ V vs. Ag/AgCl.
[b] $E_{HOMO} = -(E_{onset(ox),\ FOC} + 4.8\ \text{eV})$; $E_{LUMO} = -(E_{onset(red),\ FOC} + 4.8\ \text{eV})$.
[c] $E_g = |;\text{LUMO} - \text{HOMO}|;$.
[d] Band gaps obtained from onset absorption (λ_{onset}): $E_g^{opt} = 1240/\lambda_{onset}$.

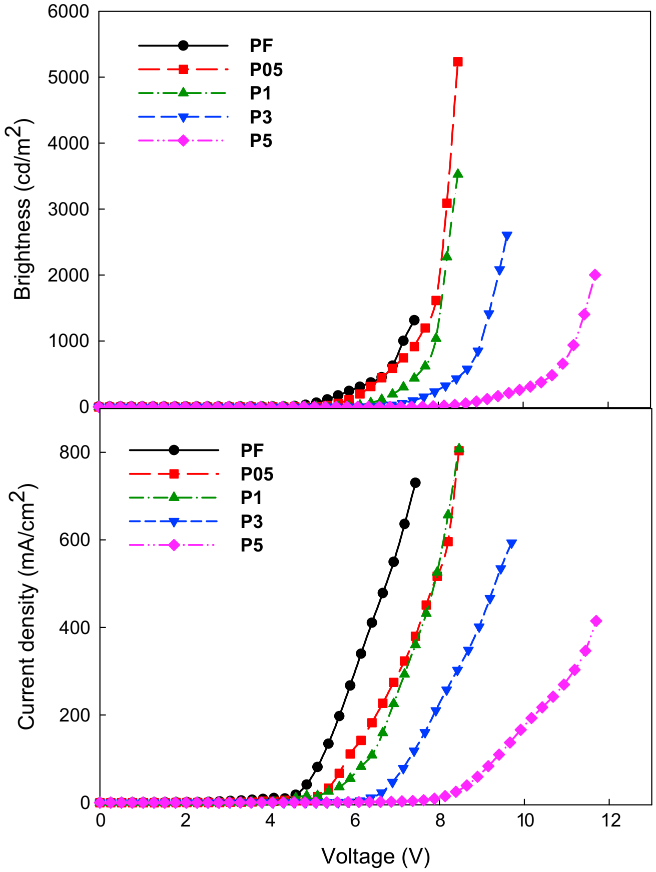

Fig. 4. Brightness–voltage and current density–voltage characteristics of the EL devices using **PF**–**P5** as emitting layer [ITO/PEDOT:PSS/polymer/Ca(50 nm)/Al (100 nm)].

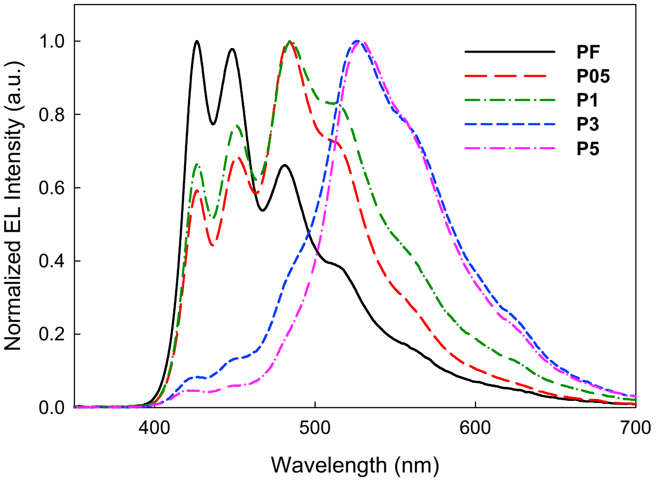

Fig. 5. Emission spectra of the electroluminescent devices using **PF** or copolyfluorenes (**P05**–**P5**) as emitting layer. Device structure: [ITO/PEDOT:PSS/polymer/Ca(50 nm)/Al (100 nm)].

Fig. 5 shows the emission spectra of the electroluminescent (EL) devices. The EL spectrum of **PF** is similar to its PL spectrum, with a major emission peak at *ca.* 429 nm. The other emission peak at 450 nm and shoulder at 484 nm correspond to $S_{10} \rightarrow S_{01}$ and $S_{10} \rightarrow S_{02}$ vibronic transitions, respectively. However, the EL spectra of **P05**–**P5** devices are obviously different from that of **PF**. The emission peaks of **P05** and **P1** shift to about 488 nm, and those of **P3** and **P5** shift further to *ca.* 530 nm. In particular, **P3** and **P5** show yellowish-green emissions because of higher **GM** composition in main chain (3.4 mol%). Moreover, the emission intensity at 400–500 nm from fluorene segments degenerates quickly with increasing **GM** contents. The overwhelming emission of **GM** chromophore (*ca.* 530 nm) in **P3** and **P5** is attributed to simultaneous energy transfer (from fluorene segments to **GM** chromophores) and charge trapping in **GM** chromophore. This phenomenon is coincident with the optical and electrochemical results mentioned above. However, **P05** and **P1** devices reveal both blue and green emission peaks due to incomplete energy transfer.

Table 4
Electroluminescent properties of the electroluminescent devices.

Device[a]	V_{on}[b] (V)	L_{max}[c] (cd/m^2)	LE_{max}[d] (cd/A)	Emission[e] (λ_{em}, nm)	CIE coordinates (x, y)[f]
PF	4.6	1310	0.18	429, 450, 484	(0.17, 0.11)
P05	5.3	5230	0.65	429, 453, 487	(0.18, 0.20)
P1	5.9	3530	0.43	429, 454, 488	(0.20, 0.22)
P3	6.6	2610	0.44	530, 559s	(0.30, 0.41)
P5	7.8	2000	0.48	533, 559s	(0.35, 0.52)

[a] Device structure: [ITO/PEDOT:PSS/polymer/Ca(50 nm)/Al(100 nm)].
[b] Turn-on voltage at 10 cd/m^2.
[c] Maximum luminance.
[d] Maximum luminance efficiency.
[e] Electroluminescent spectra *ca.* 1000 cd/m^2.
[f] The 1931 CIE coordinates at *ca.* 1000 cd/m^2.

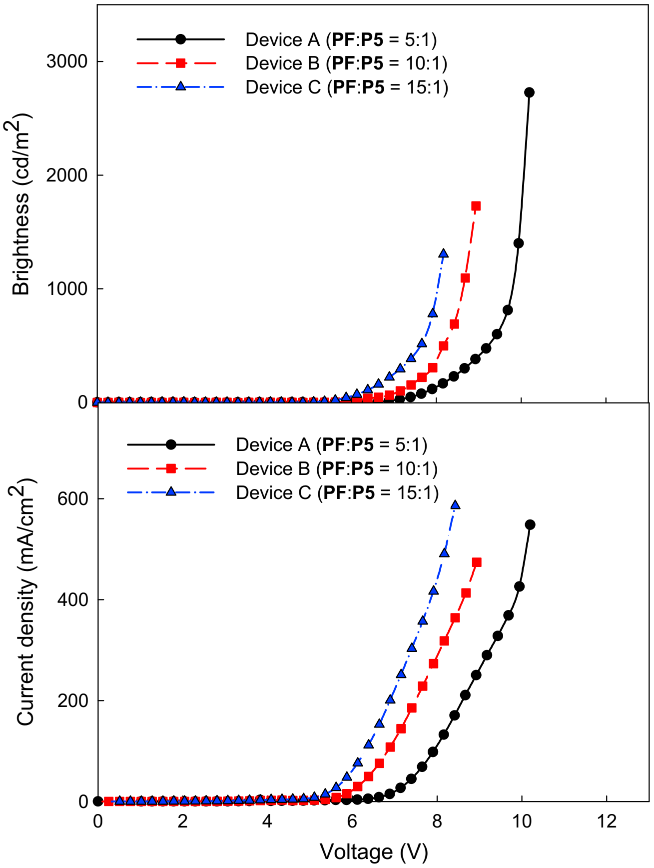

Fig. 6. Brightness–voltage and current density–voltage characteristics of the devices using blends of **PF** and **P5** as emitting layer. Device structure: [ITO/PEDOT:PSS/polymer blend/Ca(50 nm)/Al(100 nm)].

Table 5
Electroluminescent properties of blend devices.

Device[a]	Emitting layer[a] (weight ratio)	V_{on}[b] (V)	L_{max}[c] (cd/m^2)	LE_{max}[d] (cd/A)	Emission[e] (λ_{em}, nm)	CIE coordinates (x, y)[f]
A	**PF**:**P5** (5/1)	6.9	2730	0.49	429, 457, 494, 523	(0.28, 0.39)
B	**PF**:**P5** (10/1)	6.1	1730	0.36	429, 453, 491, 526	(0.26, 0.32)
C	**PF**:**P5** (15/1)	5.6	1300	0.27	429, 451, 488, 525	(0.22, 0.25)

[a] Device structure: [ITO/PEDOT:PSS/polymer blend/Ca(50 nm)/Al(100 nm)].
[b] Turn-on voltage at 10 cd/m^2.
[c] Maximum luminance.
[d] Maximum luminance efficiency.
[e] Electroluminescent spectra *ca.* 1000 cd/m^2.
[f] The 1931 CIE coordinates at *ca.* 1000 cd/m^2.

To tune the emission color by controlling the energy transfer from **PF** segments to **GM** chromophores, we fabricated EL devices using blends of **PF** and **P5** as active layer. The configuration of the blend devices was ITO/PEDOT:PSS/polymer blend/Ca (50 nm)/Al (100 nm). Fig. 6 shows the current density and brightness versus bias curves (*J*–*B*–*V*) of the blend devices (A, B, and C), with the corresponding characteristic data summarized in Table 5. The weight ratios of **PF** over **P5** in the devices A, B, and C are 5/1, 10/1, and 15/1, respectively. The maximum brightness and maximum current efficiency are 1300–2730 cd/m^2 and 0.27–0.49 cd/A respectively. The root-mean-square (rms) roughness of the blend devices (A, B, and C) was in the range of 1.43–1.5 nm that reveals no obvious phase separation. Similar molecular structures between **PF** and **P5** are probably the attribution of this phase homogeneity [42]. Moreover, the blend devices (A, B, and C) show broad emission bands at 400–700 nm (Fig. 7), in which the blue and yellowish-green emissions are attributed to the **PF** segments and **GM** chromophores respectively. The 1931 CIE coordinates of the emitted light from devices A, B, and C are (0.28, 0.39), (0.26, 0.32), and (0.22, 0.25). It is noteworthy that the CIE coordinate of device B (0.26, 0.32) appears near-white to the naked eye [21]. To conclude, the emission color of the copolyfluorenes containing **GM** chromophore can be readily tuned by controlling the chromophore contents at the synthesis stage or by simple blending with homopolyfluorene.

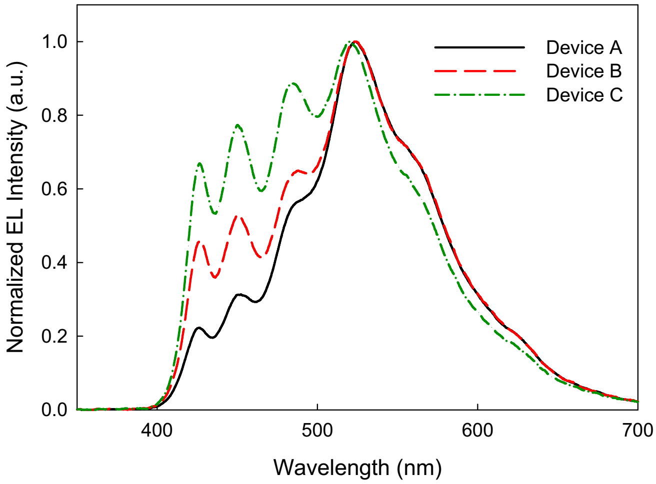

Fig. 7. Emission spectra of the EL devices using blend of **PF** and **P5** as emitting layer; Device structure: [ITO/PEDOT:PSS/polymer blend/Ca(50 nm)/Al(100 nm)]; Device A: **PF**/**P5** = 5/1, Device B: **PF**/**P5** = 10/1, Device C: **PF**/**P5** = 15/1.

4. Conclusions

We successfully synthesized a series of copolyfluorenes (**P05**–**P5**) slightly doped with 2,5-bis(2-phenyl-2-cyanovinyl) thiophene (**GM**) chromophore (0–3.4 mol%) in main chain. In solution, their absorption and PL spectra were similar to those of **PF** (peaked at 425 nm) due to low **GM** contents. However, in film state the PL spectra showed two emission peaks at *ca.* 425 nm and 535 nm attributed to fluorene segments and **GM** chromophores, respectively. The 535 nm emission intensity increased gradually with increasing **GM** contents. The electrochemical band-gap decreased from 2.87 eV to 2.75 eV with increasing **GM** contents (~3.4 mol%). Besides, the HOMO (−5.62 eV) and LUMO (−3.41 eV) of **GM** chromophore were within those of **PF** (−5.66 eV, −2.73 eV), suggesting that **GM** acts as a charge trapping sites when used as active layer in an EL device. The **P05**–**P5** revealed electroluminescent performance (2000–5230 cd/m^2, 0.43–0.65 cd/A) superior to **PF** (1310 cd/m^2, 0.18 cd/A), indicating that **GM** chromophore efficiently improves the charge recombination. Moreover, near-white-light-emitting devices were realized by blending the **P5** with **PF** (*w*/*w* = 10/1), with the CIE coordinates being (0.26, 0.32). Slight incorporation of **GM** chromophore into polyfluorene is an effective way to improve EL performance.

Acknowledgment

The authors thank the National Science Council of Taiwan for the financial aid through project NSC 98-2221-E-006-002-MY3.

Appendix. Supplementary data

Supplementary data associated with this article can be found in the on-line version, at doi:10.1016/j.polymer.2010.02.012.

References

[1] Burroughes JH, Bradley DDC, Brown AR, Marks RN, Mackay K, Friend RH, et al. Nature 1990;347(6293):539–41.
[2] Friend RH, Gymer RW, Holmes AB, Burroughes JH, Marks RN, Taliani C, et al. Nature 1999;397(6715):121–8.
[3] Zhang XJ, Shetty AS, Jenekhe SA. Macromolecules 1999;32(22):7422–9.
[4] Roncali J. Chem Rev 1992;92(4):711–38.
[5] Grem G, Leditzky G, Ullrich B, Leising G. Adv Mater 1992;4(1):36–7.
[6] Pei QB, Yang Y. J Am Chem Soc 1996;118(31):7416–7.
[7] Andersson MR, Berggren M, Inganas O, Gustafsson G, Gustafssoncarlberg JC, Selse D, et al. Macromolecules 1995;28(22):7525–9.
[8] Roncali J. Chem Rev 1997;97(1):173–205.
[9] Rothe C, Hintschich S, Monkman AP, Svensson M, Anderson MR. J Chem Phys 2002;116(23):10503–7.
[10] Burrows HD, de Melo JS, Serpa C, Arnaut LG, Monkman AP, Hamblett I, et al. J Chem Phys 2001;115(20):9601–6.
[11] Inganäs O, Granlund T, Theander M, Berggren M, Andersson MR, Ruseckas A, et al. Opt Mater 1998;9(1–4):104–8.
[12] Pei J, Yu WL, Huang W, Heeger AJ. Macromolecules 2000;33(7):2462–71.
[13] Liu B, Niu YH, Yu WL, Cao Y, Huang W. Synth Met 2002;129(2):129–34.
[14] Granlund T, Theander M, Berggren M, Andersson M, Ruzeckas A, Sundstrom V, et al. Chem Phys Lett 1998;288(5–6):879–84.
[15] Pei J, Yu W-L, Huang W, Heeger AJ. Chem Commun 2000;17:1631–2.
[16] Hsieh B-Y, Chen Y. J Polym Sci Part A Polym Chem 2009;47(3):833–44.
[17] Pal B, Yen W-C, Yang J-S, Su W-F. Macromolecules 2007;40(23):8189–94.
[18] Charas A, Morgado J, Martinho JMG, Alcáer L, Cacialli F. Synth Met 2002;127(1–3):251–4.
[19] Lim E, Jung B-J, Shim H-K. Macromolecules 2003;36(12):4288–93.
[20] Yen W-C, Pal B, Yang J-S, Hung Y-C, Lin S-T, Chao C-Y, et al. J Polym Sci Part A Polym Chem 2009;47(19):5044–56.
[21] Park M-J, Lee J, Jung IH, Park J-H, Hwang D-H, Shim H-K. Macromolecules 2008;41(24):9643–9.
[22] Jeong E, Kim SH, Jung IH, Xia Y, Lee K, Suh H, et al. J Polym Sci Part A Polym Chem 2009;47(14):3467–79.
[23] Jung IH, Jung YK, Lee J, Park J-H, Woo HY, Lee J-I, et al. J Polym Sci Part A Polym Chem 2008;46(21):7148–61.
[24] Albert IDL, Marks TJ, Ratner MA. J Am Chem Soc 1997;119(28):6575–82.
[25] Cho NS, Park JH, Shim H-K. Curr Appl Phys 2006;6(4):686–90.

[26] Cho NS, Hwang DH, Lee JK, Jung BJ, Shim H-K. Macromolecules 2002;35(4):1224–8.

[27] Kim YH, Shin DC, You H, Kwon SK. Polymer 2005;46(19):7969–73.

[28] Wang F, Luo J, Chen J, Huang F, Cao Y. Polymer 2005;46(19):8422–9.

[29] Wu TY, Chen Y. J Polym Sci Part A Polym Chem 2002;40(24):4570–80.

[30] Yang Y, Pei Q, Heeger AJ. J Appl Phys 1996;79(2):934–9.

[31] Lee J, Cho NS, Lee SK, Shim H-K. Synth Met 2005;155(1):73–9.

[32] Coulson DR. Inorg Synth 1972;13:121–4.

[33] Cho NS, Hwang DH, Jung BJ, Lim E, Lee J, Shim H-K. Macromolecules 2004;37(14):5265–73.

[34] Cho HJ, Hwang DH, Lee JI, Jung YK, Park JH, Lee J, et al. Chem Mater 2006;18(16):3780–7.

[35] Ranger M, Rondeau D, Leclerc M. Macromolecules 1997;30(25):7686–91.

[36] Yu J-M, Chen Y. J Polym Sci Part A Polym Chem 2009;47(12):2985–95.

[37] Liao C-F, Hsieh B-Y, Chen Y. J Polym Sci Part A Polym Chem 2009;47(1):149–60.

[38] Rusling JF, Suib SL. Adv Mater 1994;6(12):922–30.

[39] Liu Y, Liu MS, Jen AK-Y. Acta Polym 1999;50(2–3):105–8.

[40] Janietz S, Bradley DDC, Grell M, Giebeler C, Inbasekaran M, Woo EP. Appl Phys Lett 1998;73(17):2453–5.

[41] Herguch P, Jiang XZ, Liu MS, Jen AK-Y. Macromolecules 2002;35(16):6094–100.

[42] Zhou Y, Sun Q, Tan Z, Zhong H, Yang C, Li Y. J Phys Chem C 2007;111(18):6862–7.